



A numerical analysis for CO₂ recovery from aqueous absorbent solution by hollow fiber membrane contactor

Jeongsik Oh, Dongjae Jeong, Ina Yum, Yongtaek Lee*

*Department of Chemical Engineering, Chungnam National University, 220 Gung-dong, Yuseong-gu, Daejeon 305-764, Korea
Tel. +82428215686; Fax +8242 8228995; email: ytleee@cnu.ac.kr*

Received 1 August 2009; accepted 27 November 2009

ABSTRACT

A novel theoretical analysis was performed to strip CO₂ from an aqueous diethanolamine (DEA) solution using a membrane contactor, which is composed of porous hollow fibers. Governing equations of the system were derived for a cocurrent flow scheme of the feed absorbent steam and the permeate stream in a membrane contactor. Those were successfully solved with the proper initial conditions using a personal computer. The computer program was coded with a Compaq Visual Fortran 6.6. The concentration of free DEA and the flow rate of the recovered CO₂ in the permeate could be obtained in terms of the fiber length with changing several operating parameters: temperature in a feed, fractional reaction yield of DEA, feed flow rate and pressure in a permeate.

Keywords: Separation; Carbon dioxide; Hollow fiber contactor; Numerical analysis

1. Introduction

Many research efforts have been devoted to control the emission of the greenhouse gases: carbon dioxide, and gases described elsewhere [1]. Those gases were thought to cause the change of the global climate. It is important to capture and separate CO₂ with the proper technologies: cryogenic method, absorption, adsorption, membrane separation, and so on.

The absorption of CO₂ is known to be one of the most efficient technologies to capture CO₂ from the various sources. After capture of CO₂, the absorbent has to be regenerated so that it is reused for absorption of CO₂. As a conventional technology, a packed tower has been utilized to strip the captured carbon dioxide. However, such a process usually requires a large energy consumption. As one of the alternative

technologies to save the required energy, a membrane contactor may be a suitable candidate for separation of CO₂ from the aqueous absorbent which already absorbs CO₂ up to its equilibrium, because it provides quite large surface area per unit volume compared to the conventional packed tower [1]. A membrane contactor has been applied to absorb a gas from its mixture due to the same reason described above. In addition to the high surface ratio to the unit volume, its other advantages have been reported in elsewhere [1].

In this study, a porous membrane contactor was adopted to strip CO₂ from its aqueous diethanolamine (DEA) solution as an absorbent. In the membrane contactor, CO₂ is to be separated and collected in a permeate stream. A theoretical analysis was performed in order to predict the separation performance of CO₂ in a given membrane contactor. A set of coupled differential equations were developed and solved using a numerical method.

*Corresponding author

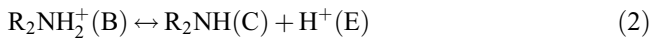
2. Theoretical analysis

Several assumptions were taken into account to develop the coupled ordinary differential equations:

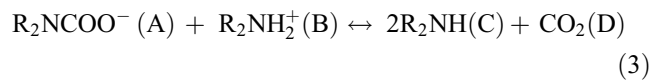
1. The absorbent liquid flows through the lumen of the membrane fiber and the permeate gas flows in the shell side with the same flow direction as the absorbent.
2. The absorbent flows as a plug flow.
3. There is no mixing along the longitudinal direction for both flows of the absorbent and the permeate.
4. There is a perfect mixing across the radial direction as in the references of [2–4].
5. The pressures of the permeate and the absorbent are kept constant.
6. The ideal gas equation of state is applied.
7. At the interface between the aqueous absorbent and the gas, Henry's law is applied.
8. The porous membrane offers negligible resistance to gas flow as in the reference of [5].

2.1. Chemical reactions

There are two steps of chemical reactions involved between CO₂ and DEA:



The overall reaction equation can be described as follows:



The stripping reaction rate (r_{CO_2}) of CO₂ can be described as follows:

$$r_{CO_2} = k_1 C_A C_E - k_{-1} C_C C_D \quad (4)$$

The equilibrium constant of the reaction (1) can be described as follows:

$$K_{eq} = (C_C C_D)/(C_A C_E) \quad (5)$$

C_A , C_B , C_C , C_D and C_E represent the molar concentration of R₂NCOO⁻, R₂NH₂⁺, R₂NH, CO₂ and H⁺ in an aqueous absorbent liquid, respectively.

From Eqs. (4) and (5), one can get the following equation:

$$r_{CO_2} = k_{-1} K_{eq} C_A C_E - k_{-1} C_C C_D \quad (6)$$

The equilibrium constant of reaction (2) can be written as:

$$K_P = (C_C C_E)/C_B \quad (7)$$

The electroneutrality condition in an absorbent liquid can be written as follows:

$$C_A = C_B + C_E \quad (8)$$

C_E is so small that it can be neglected as follows:

$$C_A = C_B \quad (9)$$

Also, the summation of all the components that are derived from DEA leads to the following equation:

$$C_T = C_A + C_B + C_C \quad (10)$$

where C_T is the total concentration of DEA.

From Eqs. (9) and (10), C_A can be described as follows:

$$C_A = (C_T - C_C)/2 \quad (11)$$

Combining Eqs. (5)–(7) and (11) and expressing the reaction rate in terms of dissolved carbon dioxide and free amine gives [6]:

$$r_{CO_2} = k_{-1} K_{eq} K_P (C_T - C_C)^2 / (4C_C) - k_{-1} C_C C_D \quad (12)$$

2.2. Governing equations of the system

Fig. 1 shows a schematic of a hollow fiber contactor. Governing equation of the system could be derived by combining the total mole balance and the mole balance of CO₂ in a finite membrane length of Δl as shown in Fig. 2.

In Fig. 2, D_i means the inner diameter of the membrane fiber. l represents the length from the inlet point

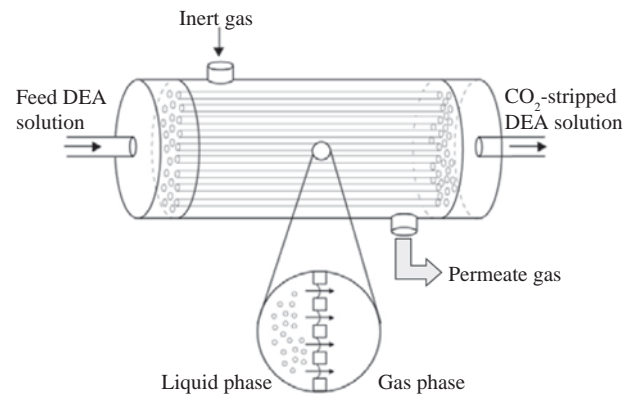


Fig. 1. A schematic of hollow fiber membrane contactor.

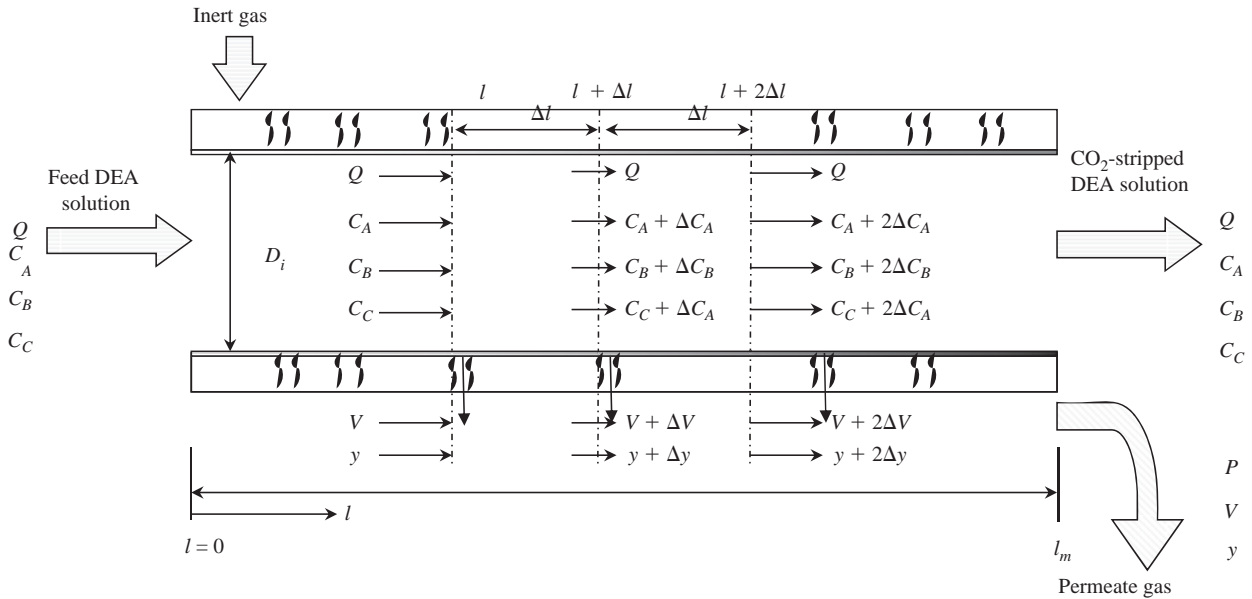


Fig. 2. A schematic of co-current flow in porous hollow fiber membrane contactor.

of the absorbent liquid. y denotes the mole fraction of CO_2 in a permeate gas. V is the total molar flow rate of the permeate stream. Q represents the flow rate of the feed in which both free DEA and DEA- CO_2 complex exist. When Q varies, the molar flow rate of free DEA and DEA- CO_2 complex are also changed. P denotes the pressure in the shell side and normally in a vacuum state. When P is adjusted, the partial pressure of CO_2 is also changed, affecting the CO_2 concentration at the vapor-liquid interface leading to the change of the driving force. The stripping rate can be controlled using a temperature as well as the CO_2 partial pressure in the gas phase.

2.2.1. Governing equation of the system in the liquid phase

The differential mole balance of free amine of R_2NH in a finite membrane length of Δl can be described according to the stoichiometric ratio of the reaction rate as follows:

$$QC_C|_{l=l+\Delta l} - QC_C|_{l=l} = (\pi D_i^2/4) \Delta l \cdot 2r_{\text{CO}_2} \quad (13)$$

Dividing each term by Δl , taking $\lim_{\Delta l \rightarrow 0}$ and rearranging Eq. (13) results in Eq. (14):

$$dC_C/dl = \{\pi D_i^2/(2Q)\} \cdot r_{\text{CO}_2} \quad (14)$$

Substituting Eq. (12) into Eq. (14) and rearranging results in Eq. (15):

$$dC_C/dl = (\pi D_i^2/2Q) \cdot \left[\frac{\{k_{-1}K_{\text{eq}}K_P(C_T - C_C)^2\}}{(4C_C)} - k_{-1}C_C C_D \right] \quad (15)$$

2.2.2. Governing equations of the system in the gas phase

The differential mole balance of V in a finite membrane length of Δl can be described as follows:

$$V|_{l=l+\Delta l} - V|_{l=l} = (\pi D_i^2/4) \Delta l \cdot r_{\text{CO}_2} \quad (16)$$

Dividing each term by Δl , taking $\lim_{\Delta l \rightarrow 0}$ and rearranging Eq. (16) results in Eq. (17):

$$dV/dl = (\pi D_i^2/4) \cdot r_{\text{CO}_2} \quad (17)$$

Substituting Eq. (12) into Eq. (17) and rearranging results in Eq. (18):

$$dV/dl = (\pi D_i^2/4) \cdot \left[\frac{\{k_{-1}K_{\text{eq}}K_P(C_T - C_C)^2\}}{(4C_C)} - k_{-1}C_C C_D \right] \quad (18)$$

The differential mole balance of CO_2 in a finite membrane length of Δl can be described as follows:

$$Vy|_{l=l+\Delta l} - Vy|_{l=l} = (\pi D_i^2/4) \Delta l \cdot r_{\text{CO}_2} \quad (19)$$

Dividing each term by Δl , taking $\lim_{\Delta l \rightarrow 0}$ and rearranging Eq. (19) results in Eq. (20):

$$d(Vy)/dl = (\pi D_i^2/4) \cdot r_{\text{CO}_2} \quad (20)$$

Rearranging the left-hand side of Eq. (20) gives:

$$V(dy/dl) + y(dV/dl) = (\pi D_i^2/4) \cdot r_{CO_2} \quad (21)$$

Substituting Eq. (17) into Eq. (21) and rearranging results in Eq. (22):

$$(dy/dl) = \{(1-y)/V\} \cdot \{(\pi D_i^2/4) \cdot r_{CO_2}\} \quad (22)$$

Substituting Eq. (12) into Eq. (22) and rearranging results in Eq. (23):

$$(dy/dl) = \{(1-y)/V\} \cdot (\pi D_i^2/4) \cdot \{[k_{-1}K_{eq}K_P(C_T - C_C)^2 / (4C_C)] - k_{-1}C_C C_D\} \quad (23)$$

2.2.3. Dimensionless equations

Equations (15), (18) and (23) can be rearranged so that they are converted to the dimensionless equations as follows:

Substituting Eqs. (33)–(35) into Eq. (15) and rearranging results in Eq. (24):

$$(C_T/l_m)/\{d(C_C/C_T)/d(l/l_m)\} = \{\pi D_i^2/(2Q)\} \cdot \{[k_{-1}K_{eq}K_P \cdot \{(C_T/C_T) - (C_C/C_T)\}^2 \cdot C_T^2]/\{4(C_C/C_T) \cdot C_T\} - \{k_{-1}(C_C/C_T) \cdot (C_D/C_T) \cdot C_T^2\}\} \quad (24)$$

Rearranging Eq. (24) results in Eq. (25):

$$dC_C^*/dl^* = [\{\pi D_i^2 l_m/(2Q)\} \cdot (k_{-1}K_{eq}K_P/4) \cdot \{(1 - C_C^*)^2 / C_C^*\} - \{\pi D_i^2 l_m k_{-1} C_T/(2Q)\} \cdot (C_C^* C_D^*)] \quad (25)$$

Substituting Eqs. (37) and (38) into Eq. (25) and rearranging results in Eq. (26):

$$dC_C^*/dl^* = \alpha \cdot \{(1 - C_C^*)^2 / C_C^*\} - \beta \cdot (C_C^* C_D^*) \quad (26)$$

Substituting Eqs. (33)–(36) into Eq. (18) and rearranging results in Eq. (27):

$$\{(QC_T/2)/l_m\} \cdot [d\{V/(QC_T/2)\}/d(l/l_m)] = (\pi D_i^2/4) \cdot \{[k_{-1}K_{eq}K_P \cdot \{(C_T/C_T) - (C_C/C_T)\}^2 \cdot C_T^2]/\{4(C_C/C_T) \cdot C_T\} - \{k_{-1}(C_C/C_T) \cdot (C_D/C_T) \cdot C_T^2\}\} \quad (27)$$

Rearranging Eq. (27) results in Eq. (28):

$$dV^*/dl^* = [\{\pi D_i^2 l_m/(2Q)\} \cdot (k_{-1}K_{eq}K_P/4) \cdot \{(1 - C_C^*)^2 / C_C^*\} - \{\pi D_i^2 l_m k_{-1} C_T/(2Q)\} \cdot (C_C^* C_D^*)] \quad (28)$$

Substituting Eqs. (37) and (38) into Eq. (28) and rearranging results in Eq. (29):

$$dV^*/dl^* = \alpha \cdot \{(1 - C_C^*)^2 / C_C^*\} - \beta \cdot (C_C^* C_D^*) \quad (29)$$

Substituting Eqs. (27)–(30) into Eq. (23) and rearranging results in Eq. (30):

$$\{dy/d(l/l_m)\}/l_m = [(1-y)/\{V/(QC_T/2)\} \cdot \{(QC_T/2)\}] \cdot (\pi D_i^2/4) \cdot \{[k_{-1}K_{eq}K_P \cdot \{(C_T/C_T) - (C_C/C_T)\}^2 \cdot C_T^2]/\{4(C_C/C_T) \cdot C_T\} - \{k_{-1}(C_C/C_T) \cdot (C_D/C_T) \cdot C_T^2\}\} \quad (30)$$

Rearranging Eq. (30) results in Eq. (31):

$$dy/dl^* = \{(1-y)/V^*\} \cdot \{[\{\pi D_i^2 l_m/(2Q)\} \cdot (k_{-1}K_{eq}K_P/4) \cdot \{(1 - C_C^*)^2 / C_C^*\} - \{\pi D_i^2 l_m k_{-1} C_T/(2Q)\} \cdot (C_C^* C_D^*)]\} \quad (31)$$

Substituting Eqs. (37) and (38) into Eq. (31) and rearranging results in Eq. (32):

$$dy/dl^* = \{(1-y)/V^*\} \cdot [\alpha \cdot \{(1 - C_C^*)^2 / C_C^*\} - \beta \cdot C_C^* C_D^*] \quad (32)$$

where the dimensionless variables and dimensionless parameters are defined as follows:

$$l^* = l/l_m \quad (33)$$

$$C_C^* = C_C/C_T \quad (34)$$

$$C_D^* = C_D/C_T \quad (35)$$

$$V^* = V/(QC_T/2) \quad (36)$$

$$\alpha = (\pi \cdot D_i^2 \cdot l_m \cdot k_{-1} \cdot K_{eq} \cdot K_P)/(8Q) \quad (37)$$

$$\beta = (\pi \cdot D_i^2 \cdot l_m \cdot C_T \cdot k_{-1})/(2Q) \quad (38)$$

Eqs. (26), (29) and (32) are subject to the initial conditions at $l^* = 0$ as follows:

$$C_C^* = C_{C,f}^* \quad (39)$$

$$V^* = V_f^* \quad (40)$$

$$y = y_f \quad (41)$$

The initial concentration of free DEA is determined using a fractional reaction yield (S) of DEA with CO_2 . This fractional reaction yield depends on the absorption process and it is supplied as one of the input data.

$$C_{C|_{l=0}} = C_T \times \left(1 - \frac{S}{100}\right) \quad (42)$$

where S denotes the fractional reaction yield of DEA with CO_2 in %. After converting $C_{C|_{l=0}}$ to the dimensionless, this initial condition is used in Eq. (39).

The concentration of CO_2 (C_D) in a liquid can be obtained in each Δl according to the following procedure: The pressure in the permeate side is used as a boundary condition in a small node of Δl so that the CO_2 concentration in a solution at the interface can be calculated. The concentration gradient will be developed across the r -direction, resulting in a new mean concentration. Using a complete mixing assumption, this new average concentration can be obtained in each node and this concentration is used to calculate the dissociation reaction rate. The wall concentration of CO_2 is determined with the Henry's law as follows [7]:

$$p_{\text{CO}_2} = H \cdot C_D \quad (43)$$

where p_{CO_2} represents the partial pressure of CO_2 in the permeate and H denotes the Henry's constant for CO_2 . The Henry's constant can be described in terms of the temperature and the total concentration of DEA and DEA- CO_2 complex in an aqueous solution as follows [8]:

$$H_{\text{CO}_2 \text{ in solution}} = 10^{\{6.31325 - (1140/T)\}} \exp\{(1.0406 \times 10^{-4}) + (6.8433 \times 10^{-3} C_T) + (1.33633 \times 10^{-2} C_T^2) + (1.1549 \times 10^{-3} C_T^3)\} \quad (44)$$

where T is the temperature in K, C_T is represented in mol/l and $H_{\text{CO}_2 \text{ in solution}}$ is expressed in atm l/mol.

3. Calculations

A Fortran program for recovery of CO_2 was developed using the Compaq Visual Fortran 6.6 software. Governing equations of the system were thought to be an initial-value problem and they were simultaneously solved using the Euler method. Fig. 3 shows the flow diagram of the computer program. Table 1

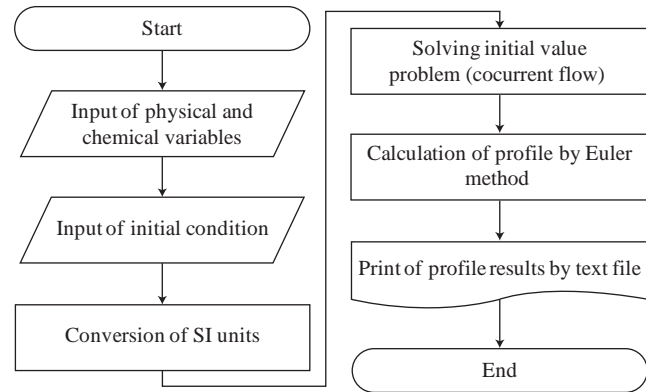


Fig. 3. Flow diagram of computer program

represents the typical characteristics of the porous hollow fiber contactor used for the computer simulation. Table 2 shows the important parameters used in the numerical analysis where the typical operating conditions were utilized as shown in Table 3.

4. Results and discussion

4.1. Effect of fractional reaction yield of DEA with CO_2 on recovery of CO_2

Figs. 4 and 5 represent the concentration of DEA converted from its complex of CO_2 in a liquid phase and the regenerated flow rate of CO_2 in a permeate as a function of the position in the membrane fiber, respectively. Both the DEA concentration and the CO_2 flow rate increase as the position in the membrane fiber is located farther from the entrance. It indicates that the DEA- CO_2 complex is dissociated and the number of free DEA molecules increases as the absorbent liquid flows along the membrane fiber. If the fractional reaction yield of DEA is high in the feed absorbent liquid, the dissociation rate of the DEA- CO_2 complex is also high, leading to the high concentration of free DEA and the large recovery of CO_2 , simultaneously. However, it is found that the concentration of free DEA at the outlet is the same, regardless of the fractional reaction yield of DEA. This may be attributed to the equilibrium limit of the dissociation reaction. It should be noted that the dissociation reaction rate is low at the

Table 1

Characteristic of the porous hollow fiber membrane contactor

Hollow fiber I.D, m	2.2×10^{-6}
Number of hollow fiber, ea	4,000
Effective length, m	0.4

Table 2
Constants used in numerical analysis

Constant	Unit	Equation ^a	Ref.
Reaction rate constant, k_{-1}	l/mol s	$\ln(k_{-1}) = 21.403 - \frac{4271.1}{T}$	[9]
Equilibrium constant, K_{eq}	–	$\log_{10}\left(\frac{1}{K_{eq}}\right) = -10.5492 + \frac{1526.27}{T}$	[10]
Equilibrium constant, K_P	mol/l	$\log_{10}(K_P) = -4.0302 - \frac{1830.15}{T} + 0.0043T$	[10]

a: The temperature (T) is expressed in K

given temperature that the DEA–CO₂ complex cannot be fully dissociated, leading to the low concentration of free DEA at the exit.

the DEA–CO₂ complex can be fully dissociated. As a result, the concentration of free DEA may be high at the low flow rate, leading to the high recovery of CO₂. When the flow rate is low, the dissociation reaction of

4.2. Effect of flow rate on recovery of CO₂

In Figs. 6 and 7, the effects of the feed flow rate are plotted on the regenerated free DEA and the recovered flow rate of CO₂. As the feed flow rate increases, both the dimensionless concentration of free DEA and the dimensionless flow rate of CO₂ decrease. At the low flow rate, the retention time in the fiber is so long that

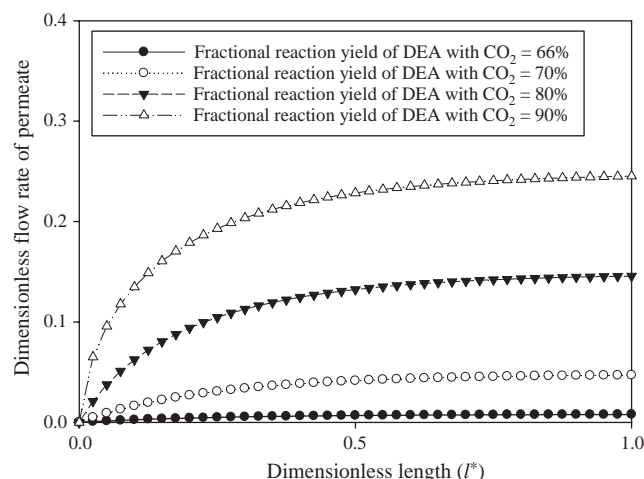


Fig. 5. Dimensionless flow rate of permeate vs. dimensionless length.

Table 3
Typical operating conditions

Variables	
Total concentration of amine in feed (C_T), mol/l	1.9258
Temperature of feed (T), K	298.15
Flow rate of feed (Q), l/s	0.00047
Pressure of shell side (P), atm	0.01
Fractional reaction yield of DEA with CO ₂ (S), %	90

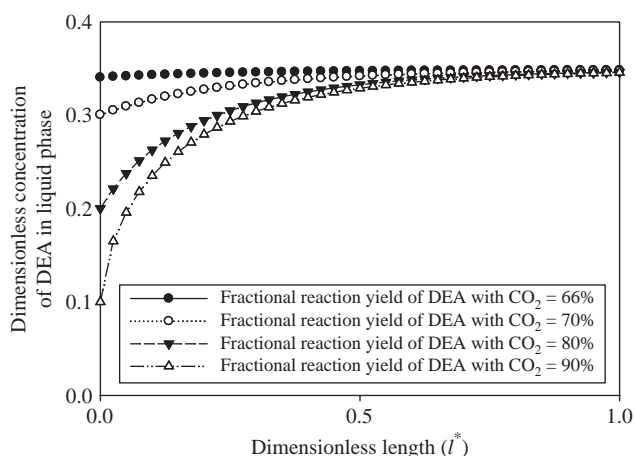


Fig. 4. Dimensionless concentration of DEA in liquid phase vs. dimensionless length.

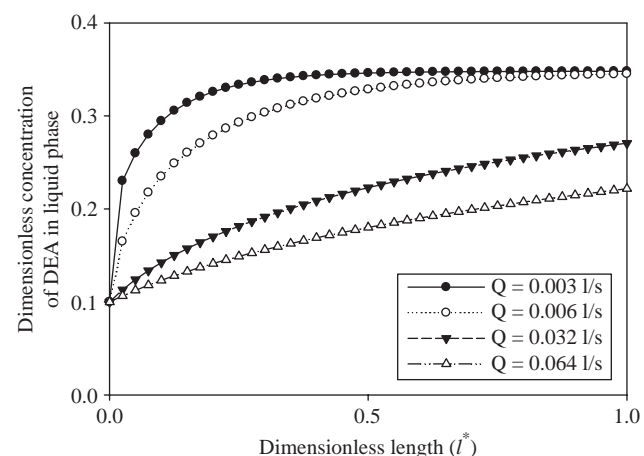


Fig. 6. Dimensionless concentration of DEA in liquid phase vs. dimensionless length.

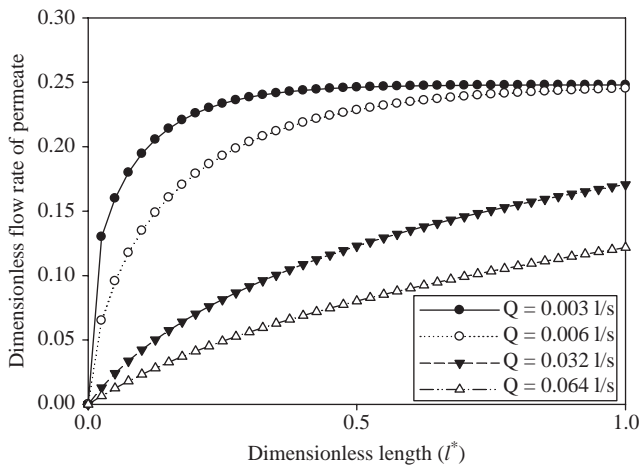


Fig. 7. Dimensionless flow rate of permeate vs. dimensionless length.

the DEA–CO₂ complex may reach the equilibrium and the concentration of free DEA converges to the constant. However, if the flow rate increases by a factor of 10, the concentration of free DEA cannot reach the equilibrium concentration even at the exit of the membrane fiber. This means that the DEA–CO₂ complex is not fully dissociated in a given fiber length. The longer fiber may be needed to regenerate completely CO₂ at the higher flow rate.

4.3. Effect of pressure in permeate side on recovery of CO₂

Figs. 8 and 9 show the effect of the pressure in the permeate side on the regenerated free DEA and the recovered flow rate of CO₂. Both the free DEA and the flow rate of the recovered CO₂ increase as the pressure in the permeate side decreases. At the low pressure in the permeate side, the interfacial concentration of CO₂

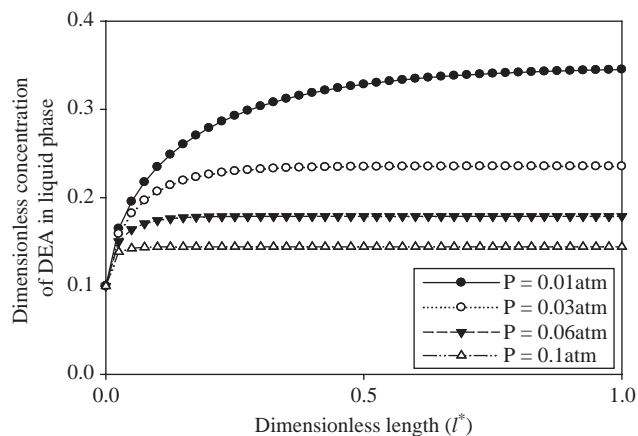


Fig. 8. Dimensionless concentration of DEA in liquid phase vs. dimensionless length.

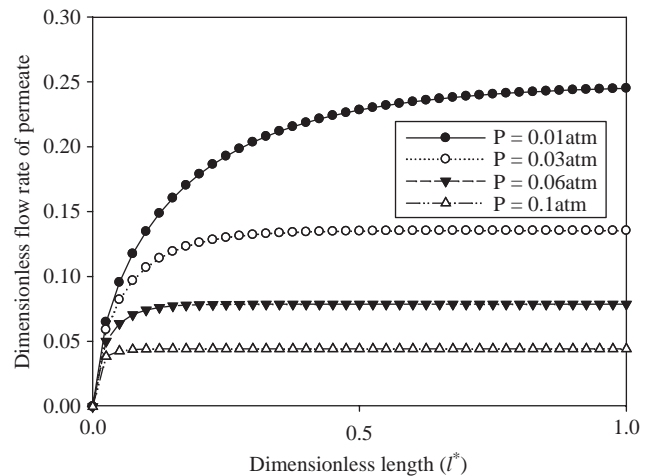


Fig. 9. Dimensionless flow rate of permeate vs. dimensionless length.

in the liquid is expected to be low according to the Henry's law. It causes the dissociation rate of the DEA–CO₂ complex to be high, leading to the high concentration of free DEA and the high flow rate of the regenerated CO₂. When the pressure in the permeate side increases by a factor of 10 from 0.01 to 0.1 atm, the recovered flow rate of CO₂ decreases by a factor of 5. It can be said that the operating pressure in the permeate side plays a very important role on the recovery of CO₂

4.4. Effect of temperature in feed on recovery of CO₂

Figs. 10 and 11 show the effect of the temperature in the feed on the regenerated free DEA and the recovered flow rate of CO₂. As the temperature increases, both the dimensionless concentration of free DEA and the dimensionless flow rate of CO₂ increase. The

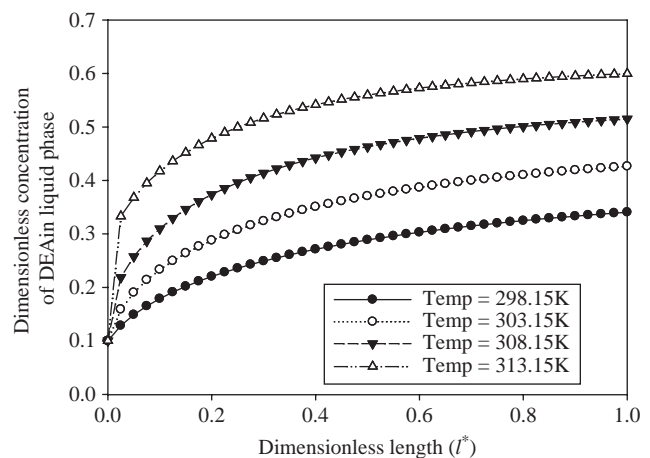


Fig. 10. Dimensionless concentration of DEA in liquid phase vs. dimensionless length.

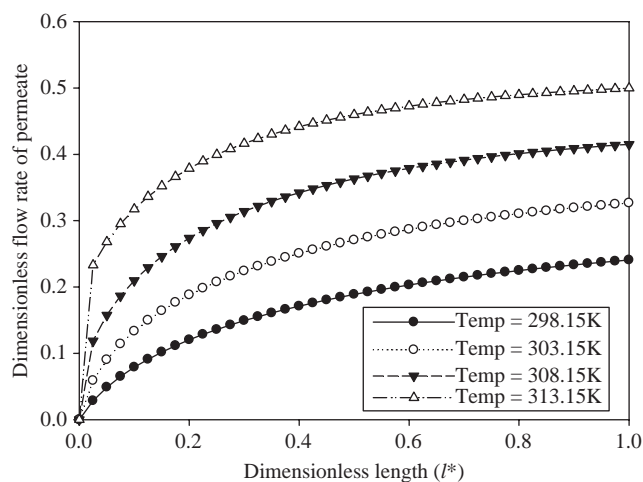


Fig. 11. Dimensionless flow rate of permeate vs. dimensionless length.

dissociation reaction rate is expected to increase as the temperature increases, leading to the increase of the flow rate of CO_2 dissociated from the DEA– CO_2 complex. As a result, the concentration of free DEA also increases. It was found that there were a few publications where the effect of the temperature was reported on the CO_2 stripping. It is believed that the high temperature may be needed to obtain the complete dissociation of DEA– CO_2 complexes.

5. Conclusions

The governing equations of the system were successfully developed to describe the stripping of CO_2 from the aqueous DEA absorbent solution in a porous membrane contactor. The reaction equation was incorporated in the governing equations of the system so that the stripping reaction rate of CO_2 could be taken into account as a function of the concentration of the associated component such as DEA, DEA– CO_2 complex and CO_2 . Governing equations of the system were numerically solved with suitable initial conditions after they were converted to the computer program in a personal computer. Along the length of the membrane fiber, those concentrations were able to be obtained, resulting in the calculation of the total flow rate of the recovered CO_2 at the outlet of the membrane contactor. It is expected that the operating conditions can be designed to obtain the suitable recovery of CO_2 .

Acknowledgement

This research was financially supported by the research program of Electrical Power R&D Foundation in Korea Institute of Energy Technology Evaluation and Planning, and partially supported by Brain Korea

21 Project of Innovative Graduate School of Energy and Environmental Materials in Daedeok Innopolis, Chungnam National University.

Symbols

C_A	Mole concentration of R_2NCOO^- in the liquid phase, mol/l
C_B	Mole concentration of R_2NH^+ in the liquid phase, mol/l
C_C	Mole concentration of R_2NH in the liquid phase, mol/l
C_D	Mole concentration of in the liquid phase, mol/l
C_E	Mole concentration of H^+ in the liquid phase, mol/l
C_T	Total amine concentration of DEA and DEA– CO_2 complex, mol/l
D_i	Inside diameter of hollow fiber, m
H	Henry's constant, atm l/mol
k_1	Forward reaction rate constant of Eq. (1), 1/mol s
k_{-1}	Backward reaction rate constant of Eq. (1), 1/mol s
K_{eq}	Equilibrium constant of Eq. (1)
K_p	Equilibrium constant of Eq. (2), mol/l
l	Length from module entrance, mm
l_m	Total length of hollow fiber contactor, mm
P	Pressure of permeate side, atm
Q	Flow rate of feed, l/s
r_{CO_2}	Chemical reaction rate, mol/l s
S	Fractional reaction yield of DEA with CO_2 , %
T	Temperature, K
V	Flow rate of permeate, mol/s
y	Mole fraction of carbon dioxide in permeate

Greek letters

α	Dimensionless parameter as defined in Eq. (37)
β	Dimensionless parameter as defined in Eq. (38)
π	Ratio of circumference of a circle to its diameter

References

- [1] P. Keshavarz, J. Fathikalajahi and S. Ayatollahi, J. Hazard. Mater., 152 (2008) 1237–1247.
- [2] M.J. Gonzalez-Munoz, S. Luquw, J.R. Alvarez and J. Coca, J. Membr. Sci., 213 (2003) 188–193.
- [3] X. He, J.A. Lie, E. Sheridan and M. Hagg, Energy Procedia, 1 (2009) 261–268.
- [4] U.V. Stockar and X. Lu, Ind. Eng. Chem. Res., 30 (1991) 1248–1257.
- [5] S. Giglia, B. Bikson, J.E. Perrin and A.A. Donatelli, Ind. Eng. Chem. Res., 30 (1991) 1239–1248.
- [6] A.K. Guha, S. Majumdar and K.H. Sirkar, Ind. Eng. Chem. Res., 29 (1990) 2093–2100.

- [7] A. Jamal, A. Meisen and C.J. Lim, *Chem. Eng. Sci.*, 61 (2006) 6571–6589.
- [8] C. Blanc and G. Demarais, *Int. Chem. Eng.*, 24 (1984) 43–52.
- [9] W.J. Ward and W.L. Bobb, *Science*, 156 (1967) 1481.
- [10] J.D. Way, R.R. Noble, D.L. Reed, G.M. Ginley and L.A. Jarr, *AIChE. J.*, 33 (1987) 480–487.
- [11] B.P. Mandal and S.S. Bandyopadhyay, *Chem. Eng. Sci.*, 60 (2005) 6438–6451.
- [12] D. Barth, C. Tondre, G. Lappal and J. Delpuech, *J. Phys. Chem.*, 85 (1981) 3660–3667.
- [13] S. Koonaphapdeelert, Z. Wu and K. Li, *Chem. Eng. Sci.*, 64 (2009) 1–8.